

Final Report for Period: 02/2010 - 01/2011**Submitted on:** 02/15/2011**Principal Investigator:** Bunz, Uwe H.**Award ID:** 0750275**Organization:** GA Tech Res Corp - GIT**Submitted By:**

Bunz, Uwe - Principal Investigator

Title:

Cruciform Fluorophores

Project Participants

Senior Personnel

Name: Bunz, Uwe**Worked for more than 160 Hours:** Yes**Contribution to Project:**

Post-doc

Name: Tolosa, Juan**Worked for more than 160 Hours:** Yes**Contribution to Project:**

Juan is paid by the EU and works as a foreign postdoc on my XF project. He prepared water soluble XFs and their interaction with surfactants.

Graduate Student

Name: McGrier, Psaras**Worked for more than 160 Hours:** Yes**Contribution to Project:**

Psaras performed the experiments for the synthesis and characterization of the tetrahydroxy-cruciform and investigated their amine-sensing properties.

Name: Zuccherro, Anthony**Worked for more than 160 Hours:** Yes**Contribution to Project:**

AJ synthesized cruciforms and investigated their interactions with silica substrates and their gas-phase sensory responses towards amines and acids.

Name: Davey, Evan**Worked for more than 160 Hours:** Yes**Contribution to Project:**

Synthesis and examination of cruciform fluorophores

Undergraduate Student

Technician, Programmer

Other Participant

Research Experience for Undergraduates

Organizational Partners

Other Collaborators or Contacts

Prof. Laren M. Tolbert (photophysical measurements)

Dr. Kyril Solntsev (postdoc Tolbert, photophysical measurements)

Prof. Christoph Fahrni (titration studies, quantum chemical calculations). In addition we have started to collaborate with Christine Payne; she looks at the biological applications of the XFs in cell staining experiments.

All of the collaborators are located at Gatech.

Activities and Findings

Research and Education Activities: (See PDF version submitted by PI at the end of the report)

see attached file.

Findings: (See PDF version submitted by PI at the end of the report)

see attached file.

Training and Development:

Psaras McGrier and AJ Zucchero have obtained their PhD. AJ works for a national security company, while Psaras (african american) is a postdoc in Fraser Stoddarts lab at Northwestern. Evan is doing his PhD with me and will defend end of 2011.

Outreach Activities:

We have a strong collaboration with Tri-cities highschool in Atlanta and we will see that we will have several high school students in our laboratory in the school year 2009/2010 and 2010/2011.

Journal Publications

McGrier, PL; Solntsev, KM; Miao, S; Tolbert, LM; Miranda, OR; Rotello, VM; Bunz, UHF, "Hydroxycruciforms: Amine-responsive fluorophores", CHEMISTRY-A EUROPEAN JOURNAL, p. 4503, vol. 14, (2008). Published, 10.1002/chem.20080029

Tolosa J., Zucchero A. J.; Bunz U. H. F., "Water-soluble cruciforms: Response to protons and selected metal ions", J. Am. Chem. Soc, p. 6498, vol. 130, (2008). Published,

AJ Zucchero, RA Shiels, PL McGrier, MA To, CW Jones, UHF Bunz., "Cruciform-Silica Hybrid Materials", Chemistry an Asian Journal, p. 262, vol. 4, (2009). Published, DOI: 10.1002/asia.200800316

Solntsev KM, McGrier PL, Fahrni CJ, Tolbert LM, Bunz UHF., "Anomalous photophysics of bis(hydroxystyryl)benzenes: A twist on the para/meta dichotomy," Org. Lett., p. 2429, vol. 10, (2008). Published,

Tolosa J, Bunz UHF., "Water Soluble Cruciforms: Effect of Surfactants on Fluorescence", Chemistry an Asian Journal, p. 270, vol. 4, (2009). Published,

Tolosa J, Zucchero AJ, Bunz UHF, "Unsymmetrical Cruciforms", J. Org. Chem., p. 523, vol. 75, (2010). Published,

Zucchero AJ, Tolosa J, Tolbert LM, Bunz UHF, "Bis(4-dibutylaminostyryl)benzene: Spectroscopic Behavior upon Protonation or Methylation", Chemistry a European Journal, p. 13075, vol. 15, (2009). Published, DOI: 10.1002/chem.200900608

Brombosz SM, Zucchero AJ, McGrier PL, "Acidochromicity of bisarylethynylbenzenes: Hydroxy versus dialkylamino substituents", Journal of Organic Chemistry, p. 8909, vol. 74, (2009). Published,

Zucchero AJ, McGrier PL, Bunz UHF, "Cross-Conjugated Cruciform Fluorophores", Accounts of Chemical Research, p. 397, vol. 43, (2009). Published,

Psaras L. McGrier, Kyril M. Solntsev, Anthony J. Zucchero, Oscar R. Miranda, Vincent M. Rotello, Laren M. Tolbert, Uwe H. F. Bunz, "Hydroxydialkylamino Cruciforms: Amphoteric Materials with Unique Photophysical Properties", Chemistry Eur. J., p. , vol. , (2011). Accepted,

Books or Other One-time Publications

Web/Internet Site

Other Specific Products

Contributions

Contributions within Discipline:

see attached file.

Contributions to Other Disciplines:

see attached file.

Contributions to Human Resource Development:

We have had excellent participation from an African American and Hispanic high school students in our project. In addition, Psaras McGrier (African American) has gone on to Postdoc and plans an academic career.

Contributions to Resources for Research and Education:

Contributions Beyond Science and Engineering:

Conference Proceedings

Categories for which nothing is reported:

Organizational Partners

Any Book

Any Web/Internet Site

Any Product

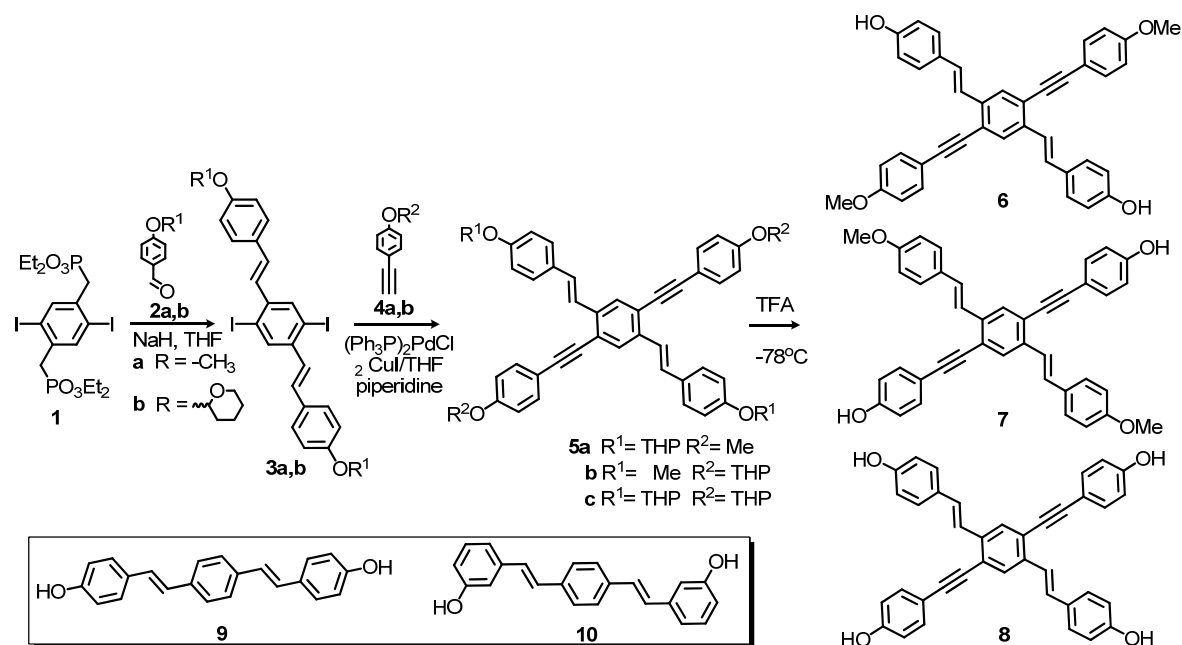
Contributions: To Any Resources for Research and Education

Contributions: To Any Beyond Science and Engineering

Any Conference

We have been successful in several different areas of synthesis and property evaluation of cruciform fluorophores (XF)s.

1) A one-molecule fluorescent library for the sensing of amines. The detection, determination and quantification of low molecular weight amines is critical in the medical field, environmental science and food safety. The enhanced presence of low molecular weight amines in breath can mark disease states in patients and in foods it indicates spoilage. We have tailored a novel class of cruciform fluorophores/chromophores (XF), 1,4-distyryl-2,5-bis(arylethynyl)benzenes, carrying phenol functionalities as model probes for amines. While these small XF-fluorophores do not display aggregation or planarization their specifically engineered frontier molecular orbitals should allow signal generation and amplification of amine-probing functions such as phenols.



Scheme 1. Synthesis of XFs **6-8** by a combination of Horner and Sonogashira methods.

We prepared the three XFs **6-8** according to Scheme 1 by a combination of Horner reaction and Sonogashira coupling. The intermediate **5c** was then deprotected by TFA to give the tetrahydro-cruciform **8**. In collaboration with Prof. Tolbert we performed a phototitration of **8**, (Figure 1), which surprisingly is not a photoacid but shows pH-dependent shifts in absorption and emission in lockstep. Upon deprotonation of **8** a significant red shift of both absorption and emission is visible. Armed with that knowledge, we exposed **8** in eight different solvents to a set of amines. Figures 2 and 3 display the results. In Figure 2 the photographed panel is shown, while Figure 3 displays a linear discriminant analysis (LDA) plot of the same data. It is interesting to note that all of the amines can be discerned by this very simple one-chromophore array.¹ To investigate this type of behavior further and extend its use, we immobilized a series of cruciform fluorophores on microstructured silica. The formed materials are highly fluorescent in the solid state and display

excellent sensitivity towards acids and bases and show concomitant changes in fluorescence color and intensity.²

In an extension of this study and to understand the photophysics of **8** better, we investigated simple bis-1,4-bis(hydroxystyryl)benzenes (*meta* and *para*, **9**, **10**)³ and their respective phenolates. While **9** displays yellow fluorescence upon deprotonation, the dianion of **10** has a more exotic photophysics that involves excitation into the S₆ state, and from there radiationless decay into the ground state. Excitation at the red-edge in the absorption spectrum of **10**⁻ revealed a

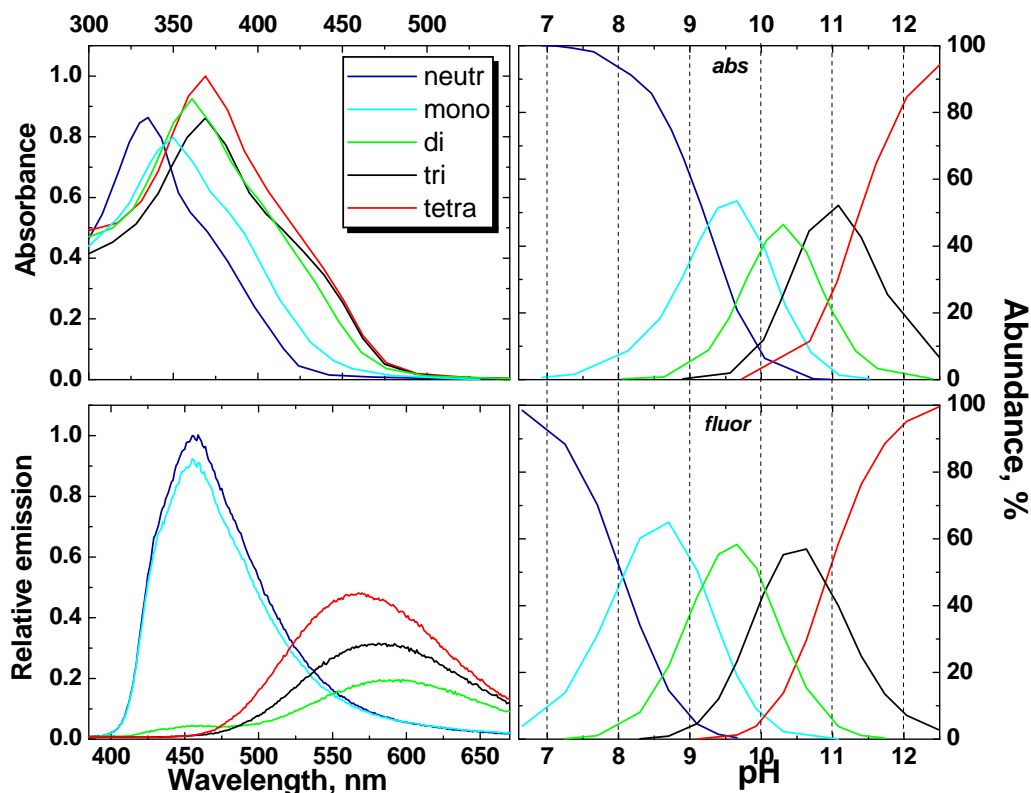


Figure 1. Deconvoluted absorption (top) and emission spectra (bottom) of the anions of **8** with relative pKa values: pKa1 = 9.2 (± 0.1); pKa2 = 10.0 (± 0.2); pKa3 = 10.6 (± 0.3); pKa4 = 11.3 (± 0.2).

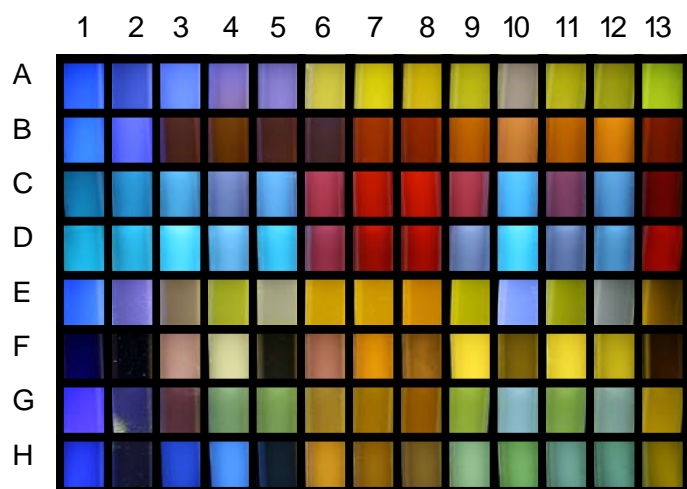


Figure 2. Photograph of solutions of **8** upon addition of amines 2-13 (left to right) 1) XF-reference, 2) histamine (6.9), 3) imidazole (6.9), 4) morpholine (8.3), 5) piperazine (9.8), 6) putrescine (9.9), 7) 1,3-diaminopropane (10.5), 8) ethylenediamine (10.7), 9) piperidine (10.8), 10) triethylamine (10.8), 11) diethylamine (11.0), 12) diisopropylamine (11.1), 13) 1,8-diazabi-cyclo[5.4.0]undec-7-ene (DBU ~12; numbers in parentheses are the pKa values of the corresponding ammonium ions in water) in different solvents (top to bottom): A) methanol, B) acetonitrile, C) DMF, D) DMSO, E) THF, F) DCM, G) ether, and H) toluene. The samples were excited using hand-held UV-lamp at an emission wavelength of 366 nm.

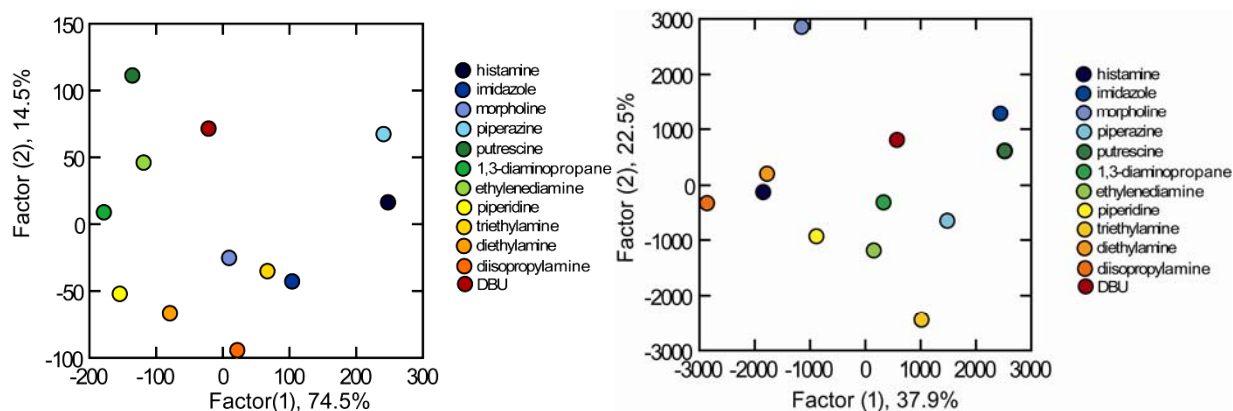
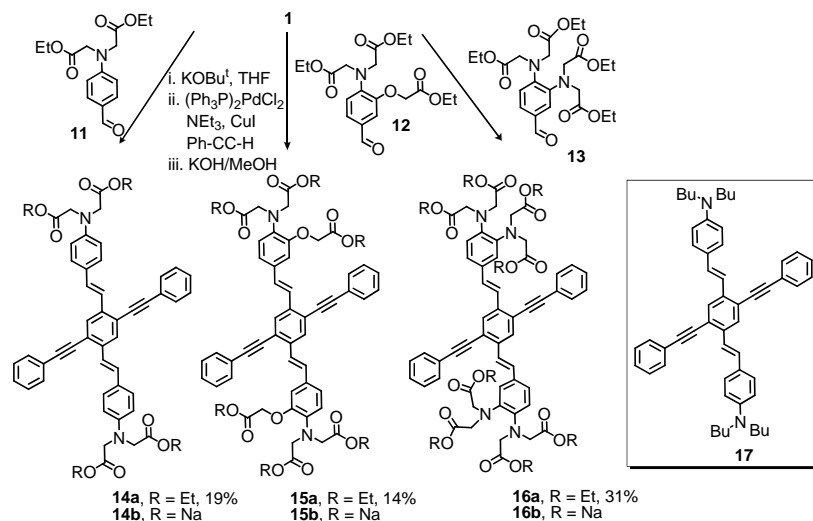


Figure 3. Linear discriminant analysis (LDA) of the differential RGB values (left) and ratio intensities (right) of **8** obtained from Figure 4, right part. The data on the left were extracted from the matrix generated by the RGB values measured for the photographs of the XF **8** dissolved in eight solvents in the presence of each different amine. The data on the right were extracted from the λ_{\max} of emission and the relative fluorescence intensities of **8** in the presence of each amine. All of the amines are separated in the 2D LDA-plot. The two factors do not represent a specific chemical property of the amines, such as pK_a value, chemical structure or other obvious chemical properties in either case.

weak emission band centered around 541 nm, which was not visible with excitation at the absorption maximum. In this case we excited the only very weakly allowed S_0 - S_1 transition. The corresponding excitation trace acquired at 541 nm peaked at 407 nm and lacked the major higher energy band visible in the absorption spectrum, thus confirming that excitation into S_6 results in non-radiative deactivation without detectible emission from S_1 .

1) Water soluble XFs. A second important issue is the synthesis of water soluble XFs as sensory materials. We have made significant inroads.⁴ The synthesis of the water soluble XFs is shown in Scheme 2. The distyrylbenzene arms contain aniline units that carry multiple acetic acid units. The photophysical properties of **14b-16b** and their metalloreactivity were examined and compared to that of the model compound **17**. It is noted that the metalloresponsive properties of **14b-16b** in aqueous buffered solution are fundamentally different from those of the model system **17** possessing the same fluorophore. While the low fluorescence quantum yields for **14b-16b** in water was not unexpected, the blue shifted emission of **15b** and **16b** in the absence of metal ions in water was surprising at first but is explained by a combination of electrostatic repulsion of the negatively charged carboxylate groups and the significant steric crowding. In the case of **15b** an attractive zinc-specific response was found, which was based upon the breakup of excimeric species (Figure 4) rather than upon the specific binding of the zinc cations to the lone pair of the aniline nitrogen in the APTRA motif of **15b**. While APTRA and similar motifs are popular and successful in the detection of metal cations in cellular environs and compartments, they may actually act not by the normally proposed coordination mechanism but also by breakup of aggregates and even, as suggested in the literature, by interaction of intact dye nanoparticles with metal cations after endocytosis into the cell. We note that the investigation of organo-soluble model compounds such as **17** is invaluable to understand the innate properties of a metallo-responsive species. The attachment of charged appendages and water as solvent fundamentally changes the fluorescent responses of XFs but

in difficult to predict ways. Without the careful investigation of **17** the interpretation of the results obtained for **14b-16b** would have been difficult and perhaps misleading.



Scheme 2. Synthesis of cruciforms **5-7** by a combination of Horner and Sonogashira methods

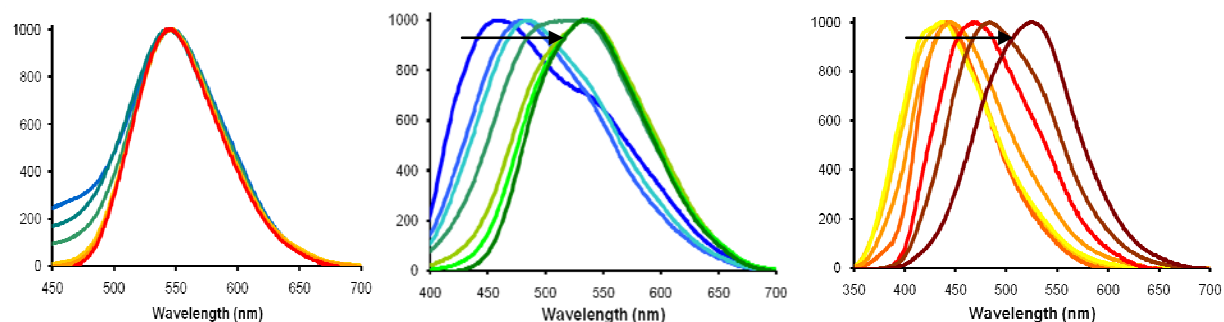


Figure 4. Emission of **14b** (left) **15b** (middle) and **16b** (right) in phosphate buffer (100 mmolL⁻¹) at 1, 2, 5, 10, 25, 50 and 100 μmolL^{-1} concentrations. The arrow displays increasing concentration of the respective cruciform.

As the low quantum yield of **14b-16b** was disappointing, we investigated ways to increase the brightness of these fluorophores in water and discovered that the addition of ionic and non-ionic surfactants led to a significant increase in fluorescence quantum yield. Particularly **15b** displayed a more than 1000-fold increase in fluorescence quantum yield (Figure 5) when exposed to Brij 35 or TritonX-100. The interaction of XFs **14b-16b** with surfactants leads to changes in their optical and luminescent behavior. A red-shift of the absorption maxima is also observed upon addition of surfactants. At the CMC the ionic surfactants have caused a significant gain in the emission intensity and beyond the CMC, the additional gain in emissive intensity is small. If interacting with nonionic surfactants, the XFs' fluorescence intensity continues to increase even when the concentration of the added surfactant is >5 x CMC. At the CMC of Triton and Brij, **15b** and **16b** display red-shifted emission, perhaps from excimeric species. Red-shifted emission is also seen for CTAB but at much lower surfactant

concentrations, which is probably due to complex formation between the positively charged CTAB and the negatively charged XFs **15b** and **16b**. The XFs **14b-16b**, display a low quantum yield in water, but a striking increase in quantum yield when they are in confined compartments such as micelles, might be of interest as “rinse-less”, i.e. background free dyes for rigid cell compartments such as the endoplasmic reticulum, cell membranes etc. that feature somewhat hydrophobic environments.⁵

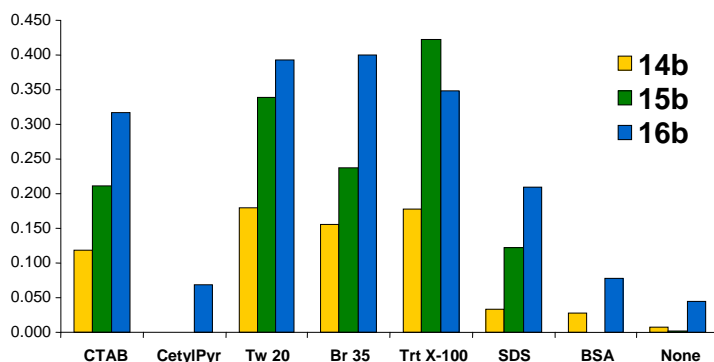


Figure 5. Quantum yields of **14b-16b** upon addition of an excess (10 mmolL^{-1} ; SDS: 100 mmolL^{-1}) of surfactants to their aqueous solution (phosphate buffer, pH 7.0, 0.1 mol L^{-1}).

Currently we are investigating the issue of excited state decomplexation and connected with it the photoacidity of hydroxy and aminocruciforms and their consanguine distyrylbenzene derivatives and see what the influence of solvent polarity and nature has on these processes.

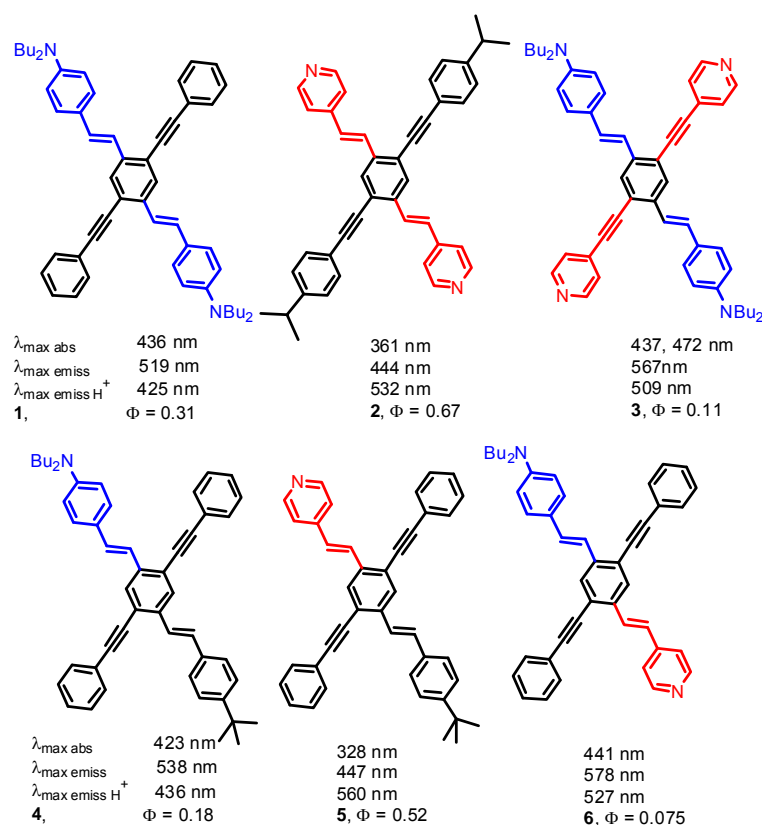
¹ Hydroxycruciforms: Amine-responsive fluorophores McGrier PL, Solntsev KM, Miao S, Tolbert LM, Miranda OR, Rotello VM, Bunz UHF *Chem. Eur. J.* 14, 4503-4510, 2008

² Cruciform-Silica Hybrid Materials (p NA), AJ Zucchero, RA Shiels, PL McGrier, MA To, CW Jones, UHF Bunz, *Chem. Asian J.* DOI: 10.1002/asia.200800316 in press.

³ Anomalous photophysics of bis(hydroxystyryl)benzenes: A twist on the para/meta dichotomy, Solntsev KM, McGrier PL, Fahrni CJ, Tolbert LM, Bunz UHF, *Org. Lett.* 10, 2429-2432, 2008

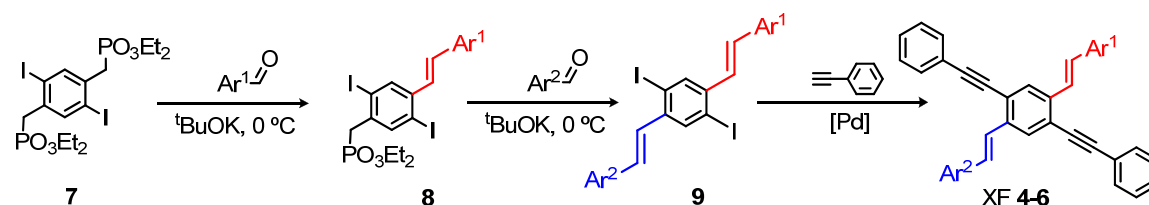
⁴ Water-soluble cruciforms: Response to protons and selected metal ions, Tolosa J, Zucchero AJ, Bunz UHF *J. Am. Chem. Soc.* 130, 6498-6506, 2008.

⁵Water Soluble Cruciforms: Effect of Surfactants on Fluorescence, Bunz UHF, Tolosa J. *Chem. Asian J.* accepted.



Unsymmetrical cruciforms: One of the important questions that we set out to investigate was the influence of the structure of the cruciforms (XF) on their optical properties. A pressing question was the comparison of the optical properties of the known symmetrical XFs **1-3**¹ with that of the unknown ones **4-6**. For the synthesis of **4-6** we developed a sequential Horner route, that started with the bisphosphonate **7**, which was reacted with 0.8 equiv. of a suitable aromatic aldehyde in the presence of potassium tert-butoxide to give the intermediates **8**. In a second step the complementary aldehyde was added to **8** in the presence of KOtBu again using a Horner reaction to give **9**. A Sonogashira coupling finishes the sequence to **4-6**.

← **Fig. 1.** Molecular structure of **1-6** and their photophysical properties recorded in dichloromethane.



Scheme 1. Synthesis of unsymmetrical XFs **4-6**.

While Fig. 1 shows the structures of **1-6** and their optical properties, Scheme 1 displays the synthetic pathways. The absorption wavelengths of the symmetrical XFs **1-3** are somewhat red-shifted compared to that of **4-6**, while the emission wavelengths of **4-6** are somewhat red-shifted from those in **1-3**, giving rise to a larger Stokes shift. Fig. 2 displays the titration of compound **4**. In the absorption we see an initial red shift upon addition of trifluoroacetic acid, and a blue shift to approx. 380 nm after addition of a large excess of TFA. In emission we observe first a blue shift (!) and then a red shift, leading to an apparent anti Stokes shift of the emission in the range of $-\log[\text{TFA}] = 4.5\text{-}3.9$. On the right hand side of Fig. 2 the fitted and deconvoluted spectra of **6** using Specfit are shown. Here we also observe a formally anti Stokes-shifted emission. Obviously that is not possible, and the explanation for this behavior is shown in Fig. 3. The critical issue is the equilibrium between the two monoprotonated species **6H⁺**. In this case, **6H⁺a** (pyridine protonated) is non-fluorescent and has a red-shifted absorption, while **6H⁺b** (aniline protonated) is blue-fluorescent with an also blue-shifted absorption. The combination of the two features then leads to the observed, counterintuitive spectroscopic features.

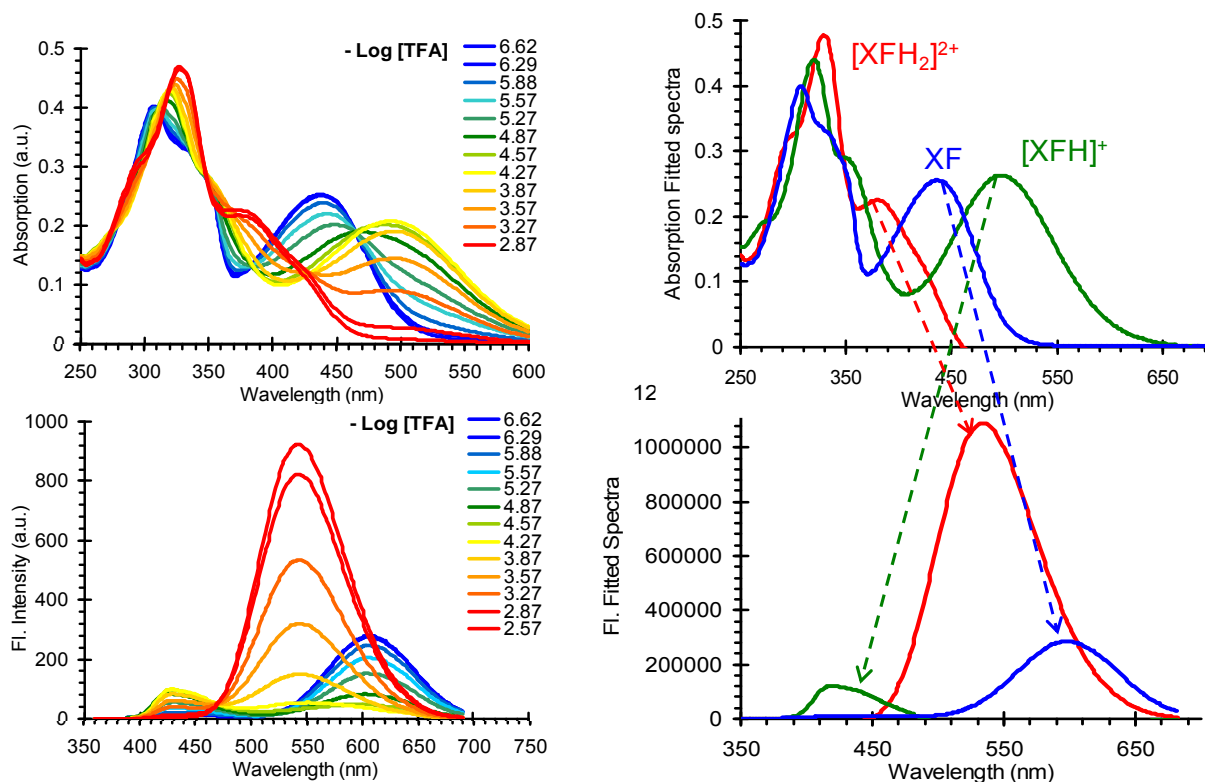
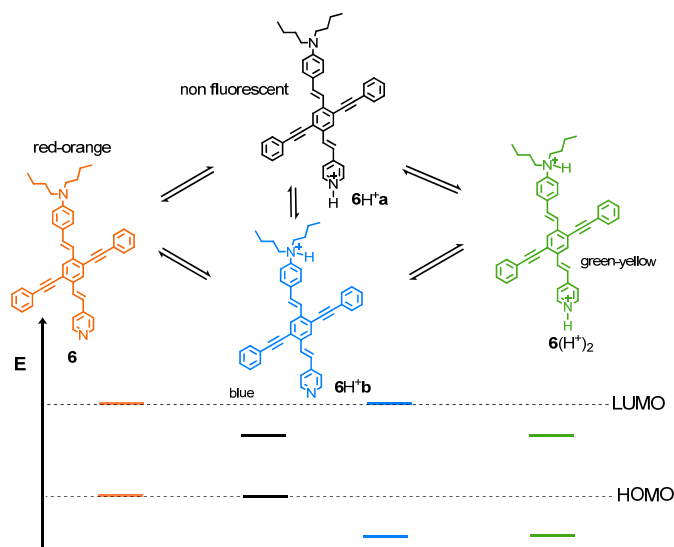


Fig. 2. Absorption and emission spectra of **6** upon titration with trifluoroacetic acid (left). Analysis of the titration of **6**. Top: Fitted UV/Vis absorption spectra. Bottom, fitted emission spectra upon exposure of **6** to trifluoroacetic acid; λ_{max} excitation = 310 nm (right).



In the occurrence of the shown equilibrium compound **6** is different from **3** where the aniline units of **3** are protonated first, featuring a blue-shifted emission. Only after full protonation of the aniline units, the pyridine units are protonated. For **6** this is apparently not the case and the juxtaposition of a pyridine and dibutylamino moieties increases the pKa of the former and lowers the pKa of the latter and makes protonation competitive.

Fig. 3. Analysis of the interaction of protons with **6**.

Cruciforms on solid supports: For the synthesis of supported fluorophores for amine sensing we decided to use commercial polystyrene beads as platform. As aldehyde-substituted beads are available, we coupled a suspension of the beads with an excess of phosphonate **7** in the presence of potassium butoxide. Our expectation was to obtain a functionalized bead with a stilbenic material featuring a free phosphonate group at the terminal. However, after the reaction was finished, we found that there were no phosphonate groups left according to IR spectroscopy. Apparently (Fig. 4) the Horner reaction led to the consumption of both phosphonate

groups under formation of ring-like structures on the beads. Further coupling to phenylacetylene under Sonogashira conditions led to the cruciforms and turned the beads into highly yellow fluorescent materials. We are currently investigating the spectroscopy (steady state and time resolved) of the beads, as the normal XFs of the same structure would be blue fluorescent. We assume that these materials form excimers and therefore show the strong yellow emission.

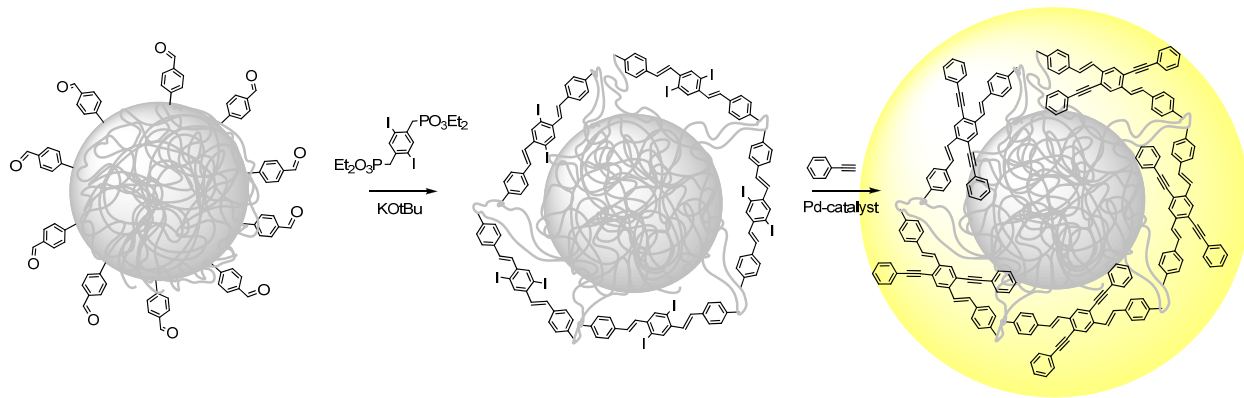


Fig. 4. Synthesis of cruciforms on beads; the case of cyclized materials.

Distyrylbenzenes and related: A central part of this proposal was the investigation of distyrylbenzenes and their photophysical properties upon protonation and metalation. The literature predicts that these materials should display excited state decomplexation of metal salts as well as enhanced photoacidity.² We investigated both issues and prepared **10-12**. The compounds **11** and **12** are obtained by partial or full methylation of **10**. We titrated **10** (Fig.s 5-7) and investigated its species distribution in emission and absorption. We found that emission and absorption change in lockstep when adding protons, and a kinetic excited state acidity could not be found. This is similar to bis(hydroxystyryl)benzene, where we also could not detect enhanced excited state acidity.³ In the case of stilbene-types,

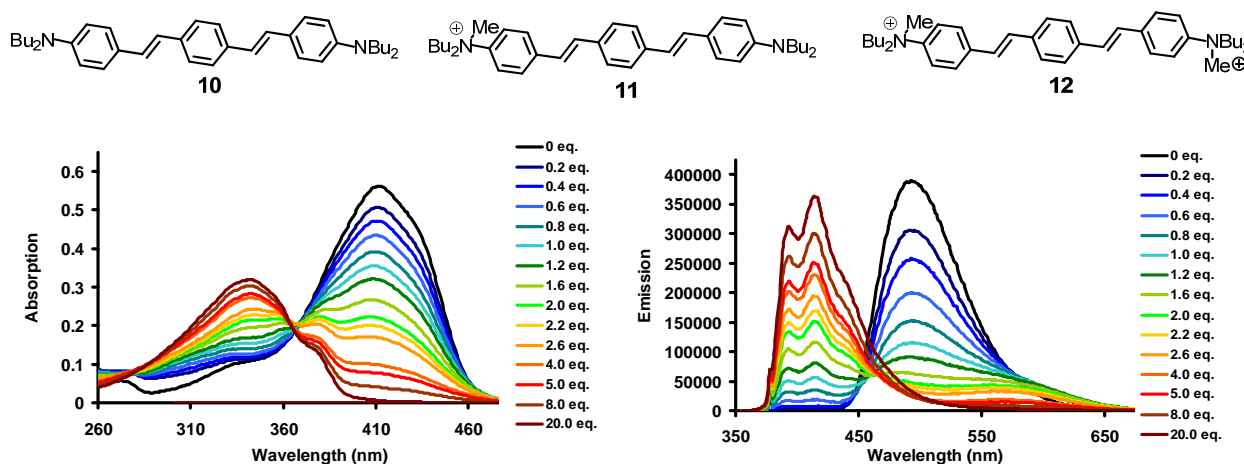


Fig. 5. Spectrophotometric titration of **10** with TFA in CH_3CN . Selected absorption (left) and emission (right) traces are shown here for clarity.

however, both excited state decomplexation as well as enhanced photoacidity has been observed for most derivatives. Our results are also different from those obtained by Marder and Perry,⁴ who investigated the metallochromicity of a series of donor-acceptor stilbenes in acetonitrile. Preliminary

Interim Report

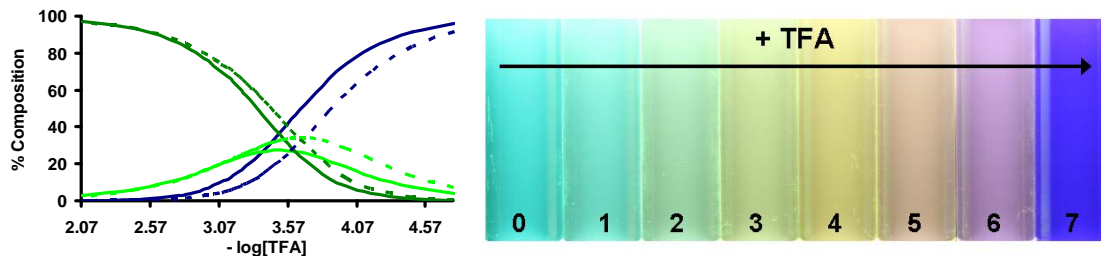


Fig. 6. SPECFIT plots derived from the absorption (solid traces) and emission (dashed traces) describing the solution composition as the TFA titration progresses. Here, the percent composition of **1** (dark blue), monoprotonated **1H⁺** (light green), and diprotonated **1(H⁺)₂** (dark green) are plotted as a function of TFA concentration. Similar profiles are obtained independently from the absorption and emission spectra. (left). Fluorescence color of **1** after addition of TFA in dichloromethane. Samples contain increasing amounts of TFA and are illuminated under blacklight ($\lambda_{\text{ex}} = 365 \text{ nm}$) (Right).

experiments using metal salts in acetonitrile also concurred with our notion that these distyrylbenzenes do not show excited state decomplexation, at least not in acetonitrile or in dichloromethane.

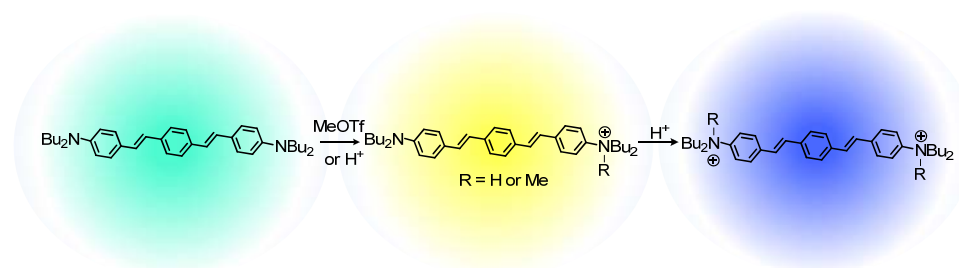


Fig. 7. Serial protonation or methylation of **10** and change in its emission color.

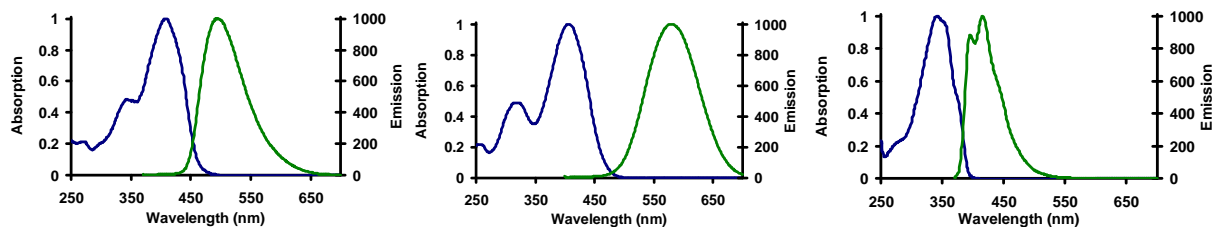


Fig. 8. Normalized absorption and emission spectra of **10**, **11**, and **12** (from left to right).

An additional fascinating issue was the intermediacy of a red-shifted species upon protonation. To investigate this issue further we prepared **11** by partial methylation of **10** using methyl triflate. Figs. 7,8 shows the results. Upon transformation into **11** the absorption does not change much, however we see a significant red shift in emission. Upon further methylation we observe significant blue shifts both in absorption and in emission. The transform of a donor-system as in **10** into a donor-acceptor system such as **11** surprisingly does not affect the absorption much but shifts the fluorescence by almost 80 nm to the red. The reason for this behavior is unclear at the moment, but should be of interest for the design of ratiometric probes that change fluorescence, but not absorption. Further planned experiments involve the synthesis of water soluble derivatives as well as the synthesis of stilbenes with

added carboxylic groups as sensory appendages to evaluate distyrylbenzene based materials that bind to metal cations in water and do not display excited state decomplexation of metal cations.

Publications during this Funding Period (year 2/3)

- [1] Unsymmetrical cruciforms, Tolosa J, Zuccherio AJ, Bunz UHF, *J. Org. Chem.* **2009**, in press.
- [2] Acidochromicity of bisarylethynylbenzenes: Hydroxy versus dialkylamino substituents, Brombosz SM, Zuccherio AJ, McGrier PL, *J. Org. Chem.* **2009**, in press.
- [3] Bis(4-dibutylaminostyryl)benzene: Spectroscopic Behavior upon Protonation or Methylation, Zuccherio AJ, Tolosa J, Tolbert LM, Bunz UHF, *Chem. Eur. J.* **2009**, Early View.
- [4] Cruciform fluorophores, Zuccherio AJ, McGrier PL, Bunz UHF, *Acc. Chem. Res.* **2009**, accepted
- [5] Cruciform-silica hybrid materials, Zuccherio AJ, Shiels RA, McGrier PL, To MA, Jones CW, Bunz UHF, *Chem. Asian J.* **4**, 262-269, **2009**
- [6] Water soluble cruciforms: Effect of surfactants on fluorescence, Tolosa J, Bunz UHF, *Chem. Asian J.* **4**, 270-276, **2009**.
- [7] Solntsev KM, McGrier PL, Fahrni CJ, Tolbert LM, Bunz UHF, *Org. Lett.* **10**, 2429-2432, **2008**.

¹ Cruciforms as functional fluorophores: Response to protons and selected metal ions Zuccherio AJ, Wilson JN, Bunz UHF *J. Am. Chem. Soc.* **128**, 11872-11881, 2006. Switching of intramolecular charge transfer in cruciforms: Metal ion sensing, Wilson JN, Bunz UHF *J. Am. Chem. Soc.* **127**, 4124-4125, 2005

² Femtosecond to Subnanosecond Multistep Calcium Photoejection from a Crown Ether-Linked Merocyanine, Ley C, Lacomat F, Plaza P, Martin MM, Leray I, Valeur B, *ChemPhysChem.* **10**, 276-281, 2009; Reversible bulk photorelease of strontium ion from a crown ether-linked merocyanine, Plaza P, Leray I, Chagnenet-Barret P, Martin MM, Valeur B *ChemPhysChem.* **3**, 668-674, 2002

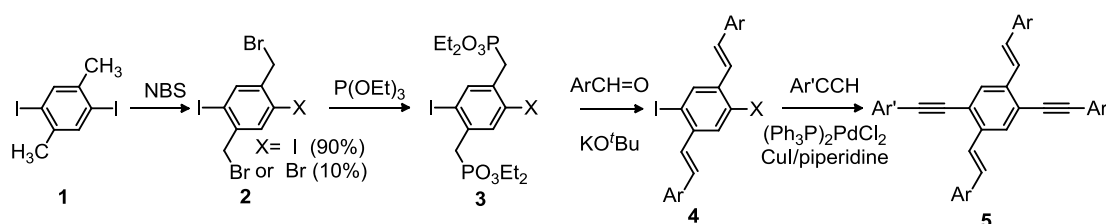
³ Anomalous photophysics of bis(hydroxystyryl)benzenes: A twist on the para/meta dichotomy, Solntsev KM, McGrier PL, Fahrni CJ, Tolbert LM, Bunz UHF *Org. Lett.* **10**, 2429-2432, 2008

⁴ Metal-ion sensing fluorophores with large two-photon absorption cross sections: Aza-crown ether substituted donor-acceptor-donor distyryl benzenes Pond SJK, Tsutsumi O, Rumi M, Kwon O, Zojer E, Bredas JL, Marder SR, Perry JW *J. Am. Chem. Soc.* **126**, 9291-9306.

Final Report for NSF CHE 0750275, Cruciforms PI Bunz

We have developed and examined the chemistry, sensory responses and photophysics of a series of different cross-shaped fluorophores, the XF **5**. These materials are highly interesting fluorescent species that display large auxochromic responses, i.e. substituent-dependent fluorescence wavelength.

Synthesis of organosoluble XFs: The symmetrical cruciforms **5** are easily synthesized in a two step scheme, starting from the bisphosphonate **3** that is reacted with a series of aldehydes in the presence of KO^tBu to give the corresponding 1,4-diiodo-2,5-distyrylbenzenes, which are further reacted in a Sonogashira coupling to give the symmetrical XFs **5** in good to excellent yields. The modular synthetic scheme allows the introduction of almost any substituent into either axis of the XF. Figure 1 displays the emission colors of the compounds **5a-f**, while Figure 2 displays the corresponding spectra.



Scheme 1. Synthesis of symmetrical XFs **5**

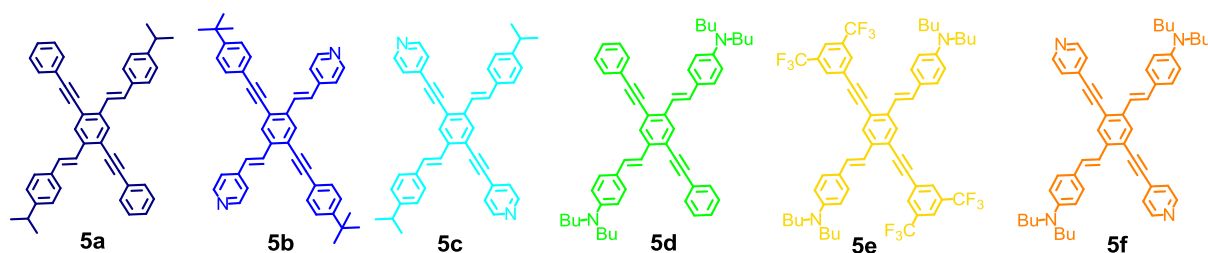


Figure 1. Emission colors of different XFs **5a-f** in dichloromethane under blacklight.

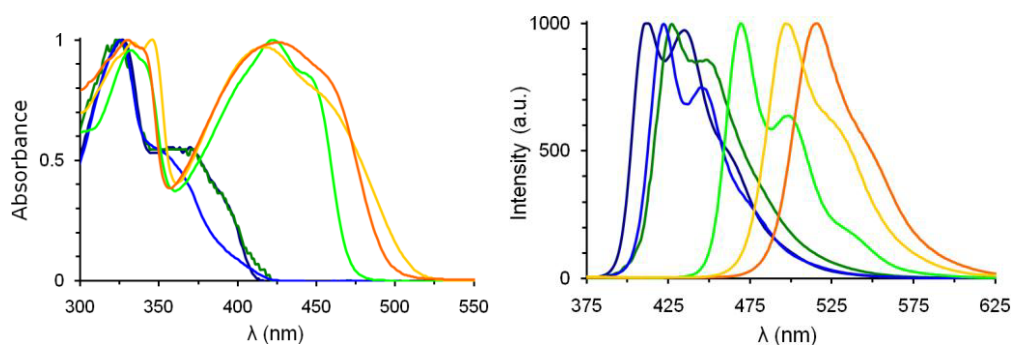
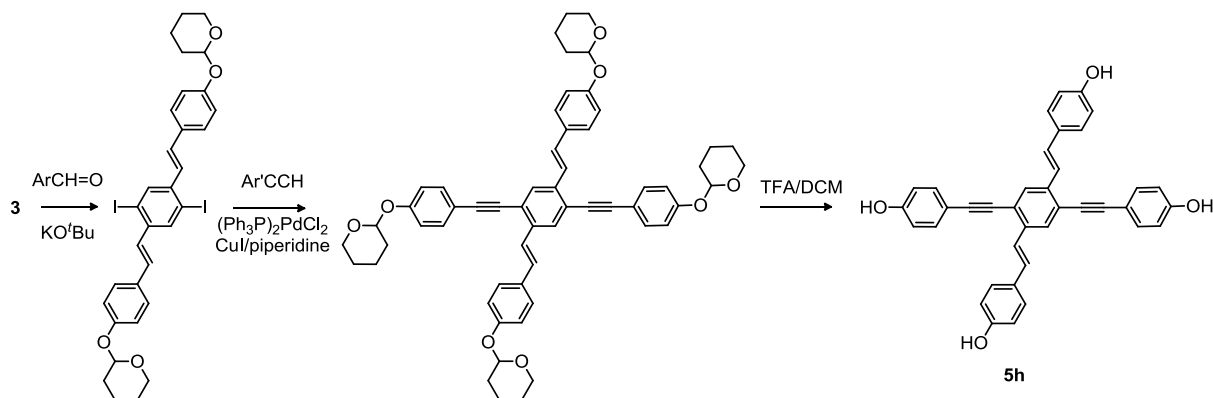


Figure 2. Normalized absorption (left) and emission (right) of XFs **5a-f** in hexanes.

Somewhat more challenging was the synthesis of the dihydroxy and tetrahydroxy XF **5g** and **5h**. In this case the aldehyde and the alkyne had to be protected, and in the last step the protecting groups were removed by trifluoroacetic acid in dichloromethane. The tetrahydroxy-XF **5h** is a yellow powder that dissolves well in polar solvents such as methanol, DMF, DMSO, acetonitrile, and somewhat in solvents such as DCM, ether and THF.



Scheme 2. Synthesis of the tetrahydroxy-XF **5h**.

As it is easily visible, the substituents have a significant influence on absorption but even more so, on the emission of the XFs **5**. The reason for the large auxochromic effects is in the orbital structure. In XFs where there is no donor-acceptor substitution, the HOMO and the LUMO are evenly distributed over the molecular skeleton. In the case of the donor-acceptor substituted **5f'**, the situation is very different (Figure 3). The HOMO is now positioned on the distyrylbenzene axis, while the LUMO is localized on the bisarylethynyl axis. This has interesting consequences, as the energy of the HOMO and the LUMO can be varied almost independently if the XFs display a significant amount of donor-acceptor character.

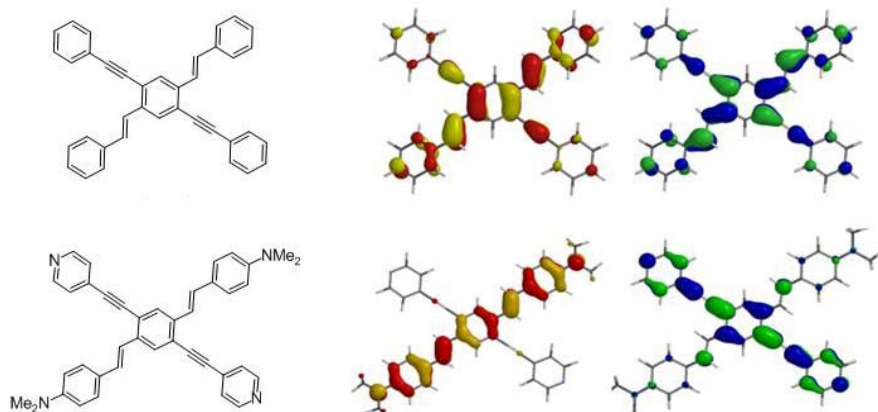


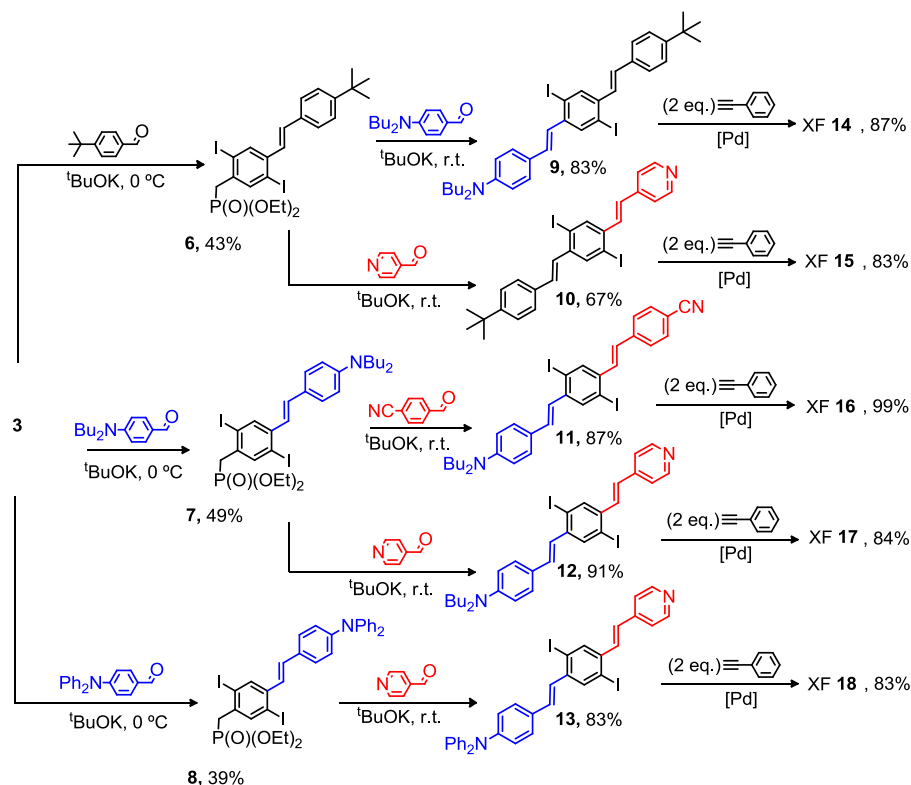
Figure 3. FMOs of XFs without substituents (top) and with donor-acceptor substituents **5f'** (bottom).

We have been able to synthesize not only symmetrical XFs, but also unsymmetrical XFs, **14-18** (Scheme 3). In this case an excess of the bisphosphonate was treated with an aldehyde in the presence of potassium butoxide to obtain the corresponding stilbenes **6-8**. After isolation the intermediates were reacted with an equivalent of the second aldehyde under addition of potassium butoxide to give the unsymmetrical distyrylbenzenes **9-13** in good to excellent yields. In the last step **9-13** were treated with phenylacetylene under Sonogashira conditions to obtain **14-18** as the XFs.

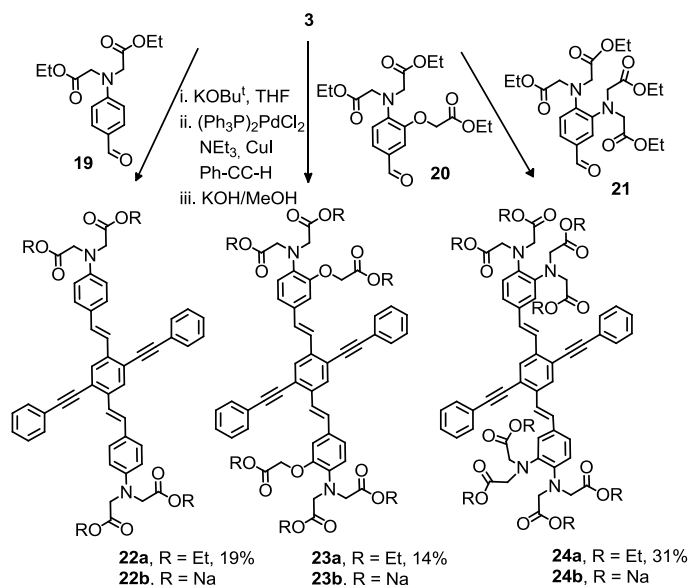
Synthesis of water soluble XFs.

For any type of sensory applications in cells or in aqueous environs, the XFs will have to show water solubility. To obtain this we prepared the building blocks **19-21** and reacted them

(Scheme 4) with the aldehydes **19-21** under addition of KOtBu. Sonogashira coupling with phenylacetylene and subsequent saponification furnish the water soluble title compounds **22b-24b** in fair to good yields.



Scheme 3. Synthesis of unymmetrical XFs **14-18**.



Scheme 4. Synthesis of water soluble XFs **22b-24b**

Properties of XFs.

Metalloresponsivity of XFs. We exposed **5f** to both TFA and Zn^{2+} . Upon addition of increasing equivalents of Zn^{2+} ions to **5f** in chloroform, a rare two-stage fluorescence response is observed: the emission color changes dramatically from orange to blue and then to green (Figure 5). A similar response is observed upon addition of TFA to **5f**. A spectrophotometric titration of **5f** with $Zn(OTf)_2$ in dichloromethane was performed (Figure 5).

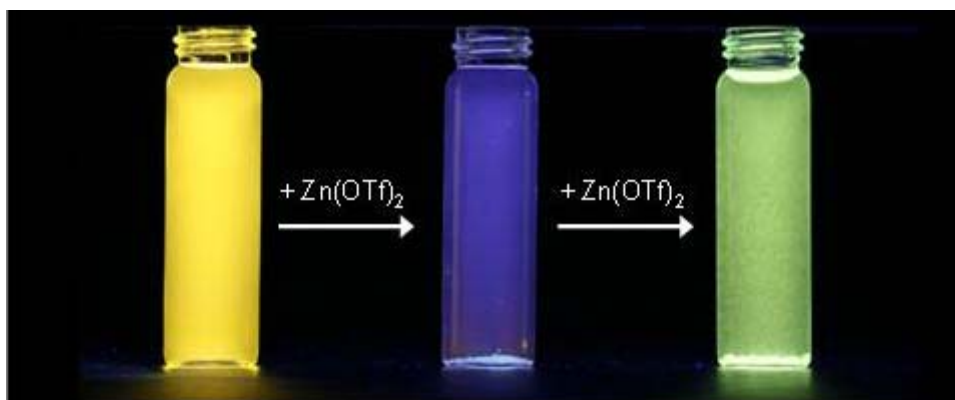


Figure 4. Emission of **5f** in chloroform (left vial, orange emission), upon addition of a small amount of $\text{Zn}(\text{OTf})_2$ (center vial, blue emission), and upon addition of a large excess of $\text{Zn}(\text{OTf})_2$ (right vial, green emission).

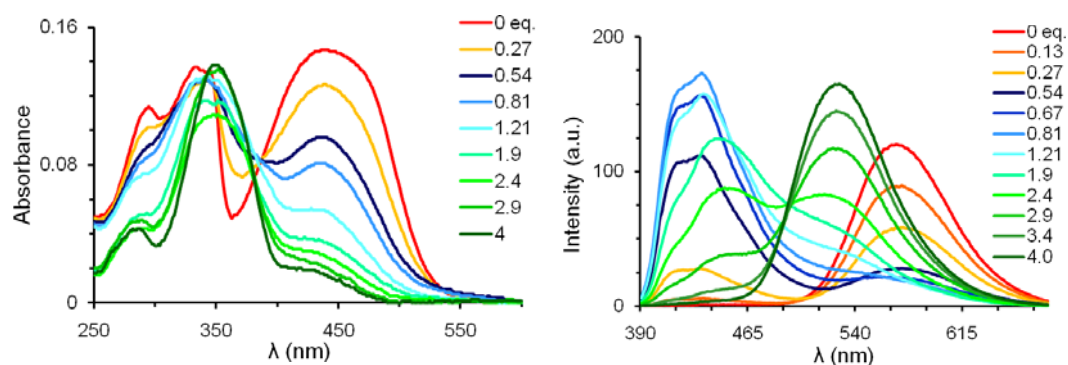


Figure 5. Absorption (left) and emission (right) of **5f** in dichloromethane upon exposure to increasing equivalents of zinc triflate.

The absorption of **5f** consists of a high energy band 335 nm and a charge transfer peak centered at 440 nm. Upon addition of Zn^{2+} , the charge transfer feature disappears accompanied by a small shift (335 \rightarrow 350 nm) in the high energy band. In the emission, upon addition of a small quantity of $\text{Zn}(\text{OTf})_2$, a large blue shift (570 \rightarrow 420 nm) occurs; subsequent addition of Zn^{2+} results in a bathochromic shift (420 \rightarrow 530 nm).

This two-stage response can be rationalized by examining the sensory response of **5d** and **5c**; these XFs are bona fide models of **5f** possessing either pyridyl or dibutylamino substituents. In the case of **5c**, only a hypsochromic shift (527 \rightarrow 430 nm) is observed upon addition of Zn^{2+} (Figure 6). Consideration of the FMO arrangement in **5c** offers an explanation; B3LYP 6-31G**//6-31G** calculations suggest the HOMO is localized primarily on the distyryl axis of the XF. Binding of Zn^{2+} to the aniline nitrogens of **5c** stabilizes the HOMO while leaving the LUMO largely unperturbed. As a result, a blue shift in emission is observed. XF **5d** contains exclusively the pyridyl binding functionalities on the arylethynyl axis. Upon reaction with zinc triflate, a redshift in emission (457 \rightarrow 564 nm) is observed (Figure 7). Zinc coordination of the pyridyl nitrogens stabilizes the LUMO of **5d** which lies along the arylethynyl axis of the XF scaffold while the HOMO is unaffected (Figure 3). The responses observed upon exposure of XFs to metal ions raises questions as to the locus and stoichiometry of analyte interaction. In the case of alkylamino-functionalized XFs, it is of interest to determine if the metal cation coordinates to the aniline nitrogen or to the electron rich π -face of the aromatic ring. In addition, it is important to determine if the sensory response results from the coordination of one or both available nitrogens on an XF branch. In the case of protons, both the stoichiometry and locus of binding are known: an excess of TFA added to **5** will protonate all available nitrogens.

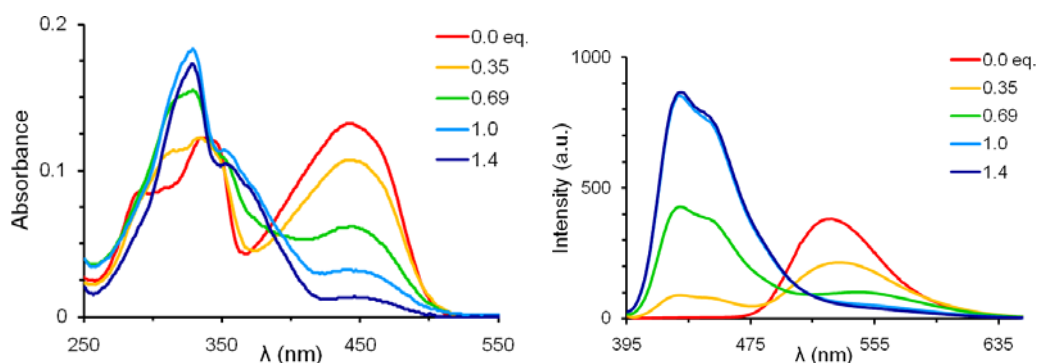


Figure 6. Absorption (left) and emission (right) of **5c** in dichloromethane upon exposure to increasing equivalents of zinc triflate.

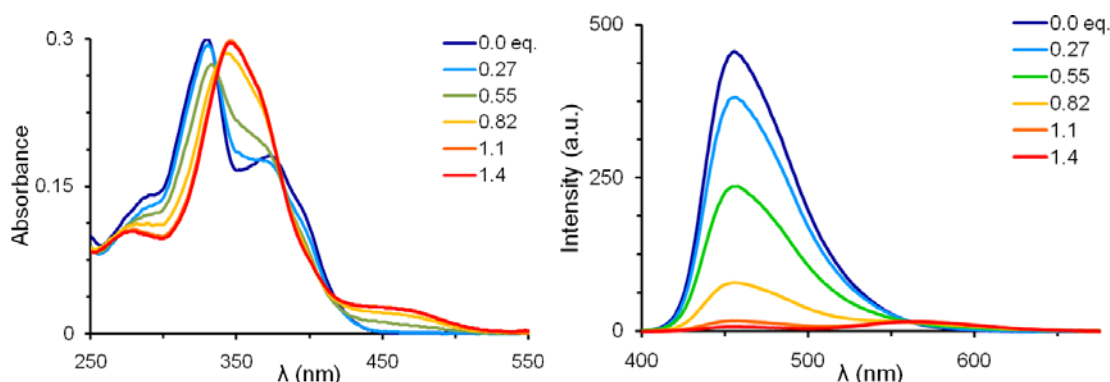
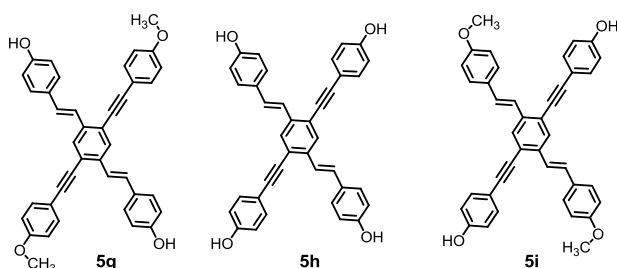


Figure 7. Absorption (left) and emission (right) of **5d** in dichloromethane upon exposure to increasing equivalents of zinc triflate.

Comparing the spectroscopic responses observed for Zn^{2+} with those found for TFA will reveal if a similar mode of analyte interaction with the XF exists. The absorption, emission, fluorescence quantum yield, and fluorescence lifetimes of **5** were measured upon addition of excess zinc triflate and trifluoroacetic acid. In all cases, *similar changes are observed in the spectroscopic properties of 5 upon addition of TFA and Zn^{2+}* . This suggests that the metal cations are coordinating through the lewis-basic nitrogens and not via the arene rings.

Response of hydroxyl-XFs towards amines



The detection and quantification of aliphatic amines is of importance in environmental science, pharmaceutical industries and dye manufacturing. They are frequent pollutants in landfills, manufacturing sites, and in the soil and aqueous environment. Biogenic amines such as histamine and putrescine are products of the enzymatic

decarboxylation of amino acids. Their presence serves as an indicator of food spoilage for fish products.³³ The detection of amines has been achieved by molecularly imprinted polymers,³⁴ enzymes,³⁵ single molecule and array sensors,³⁶ and chromatographic methods.³⁷ To further examine the potential utility of XFs as sensory cores, we examined **5g-i** possessing strategically placed phenol functionalities.

XFs **5g-i** display blue emissions (λ_{max} 450-475) and quantum yields in the range of 16-37%. Titration of **5g-i** with KOH demonstrated that in the case of **5g**, deprotonation results in a new band at 416 nm in the absorption spectra and a shift in the emission spectra (460 \rightarrow 600 nm). Deprotonation of **5i** led to quenching. Upon deprotonation of **5h**, an isosbestic point is

visible at 346 nm and absorption maximum develops at 370 nm. When traversing from pH 7 to 10 we observe a significantly red-shifted (588 nm) emission band of lower intensity. Upon further increasing the pH, the fluorescence intensity of **5h** increases again and the emission maximum blue shifts to 565 nm (Figure 8).

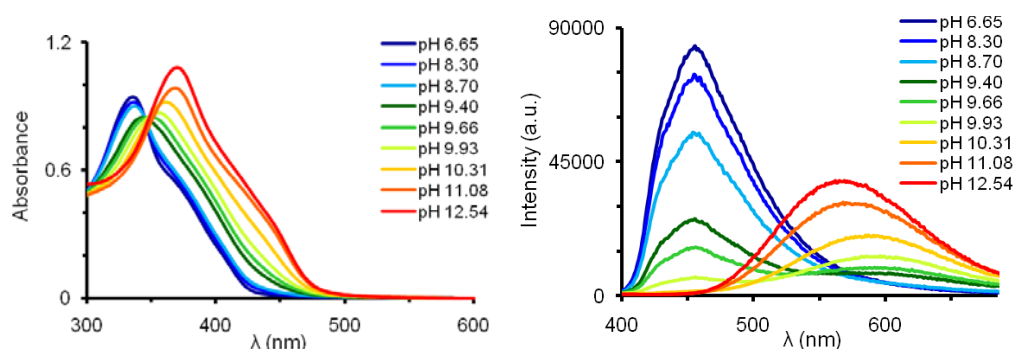


Figure 8. Spectrophotometric titration of **5h** in 2:1 MeOH/H₂O.

Solutions of **5h** were prepared in nine different solvents and representative amines were added. While some shifts in emission were observed in the case of **5g**, exposure of amines to **5h** resulted in solutions with emission colors ranging from blue to red traversing yellow and green *spanning the full visible spectral range* (Figure 9). From these observations, we concluded that the difference in pK_a between the excited hydroxycruciforms and amines is sufficient to produce a solvent-separated ion pair.³⁸ In the ground state, the observed ΔpK_a results in the formation of the hydrogen-bonded complexes. Utilizing the Kamlet-Taft method, it was determined that the increase of solvent polarity and basicity causes the bathochromic shift of the emission, while the acidity of the solvent works in the opposite direction. While it is not yet clear why each amine displays different shifts in emission, we do know that it is dependent upon the structure of the amine and the chemical environment. The results obtained for **5h** exposed to amines in varied solvents was analyzed by linear discriminant analysis (LDA) using matrices derived by simply extracting the RGB values in Figure 9 (Figure 10). Surprisingly, all 12 amines can be discerned. These experiments imply that a ‘chemical nose’ need not involve large numbers of unique sensors; rather, variable responsivity can be achieved by employing one sensor molecule in different chemical environments. We note that this phenomenon has important implications for the future design of simple yet powerful differential sensor arrays.

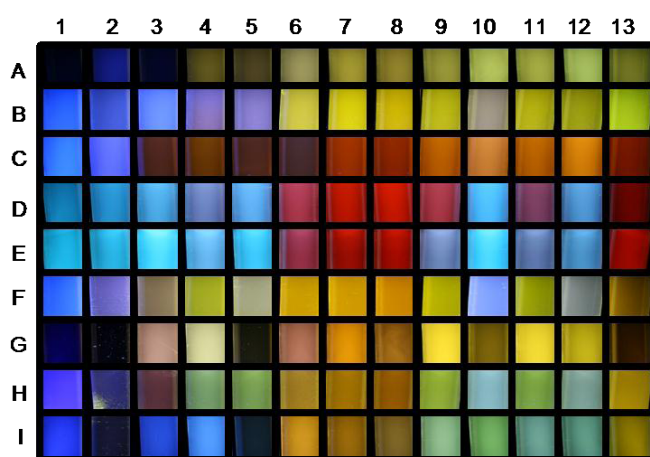


Figure 9. Photograph of solutions (λ_{max} ex = 365 nm) of **5h** upon addition of amines 2–13 (left to right) 1) **5h**, 2) histamine (6.9), 3) imidazole (6.9), 4) morpholine (8.3), 5) piperazine (9.8), 6) putrescine (9.9), 7) 1,3-diaminopropane (10.5), 8) ethylenediamine (10.7), 9) piperidine (10.8), 10) triethylamine (10.8), 11) diethylamine (11.0), 12) diisopropylamine (11.1), 13) 1,8-diazabicyclo[5.4.0]undec-7-ene (DBU ~12) [numbers in parentheses are the pK_a values of the corresponding

ammonium ions in water] in different solvents (top to bottom): A) 90:10 water/methanol B) methanol, C) acetonitrile, D) DMF, E) DMSO, F) THF, G) dichloromethane, H) diethyl ether, and I) toluene.

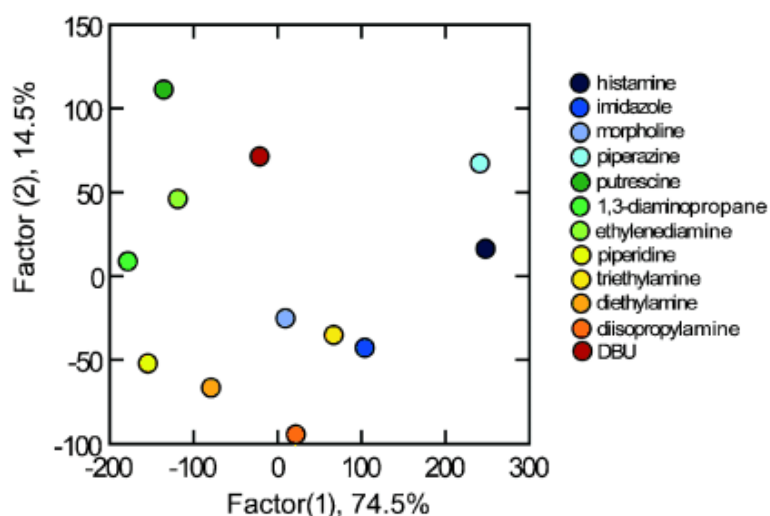


Figure 10. LDA results demonstrating the identification of 12 amines using **14** in nine solvents. The plot was extracted from the RGB values measured from the photographs of **14** with amines in nine solvents (Figure 9).

dimensional 'X-shaped' materials provides access to conjugated architectures with unexpected and exciting properties. XFs represent a prime example of such novel conjugated architectures. Donor-acceptor substitution results in materials that have been employed as building blocks in supramolecular coordination assemblies^{23,24} and used as switches in molecular electronics; however, their FMO-architecture makes these fluorophores even more seductive candidates in sensing applications as demonstrated in the case of amines.

Moving beyond one-dimensional molecular wire-type fluorophores to two-

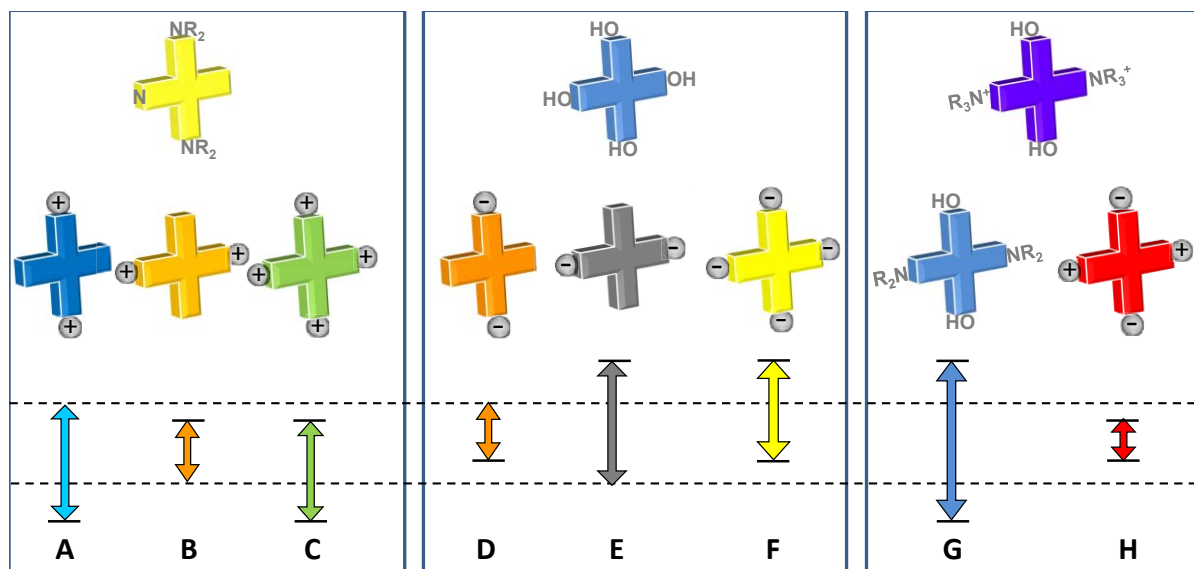


Figure 11. Schematic representation of the potential sensory responses elicited by the binding of cationic and/or anionic species to symmetrically-functionalized XFs. Eight different binding scenarios are conceivable resulting in five unique fluorescence responses. The dotted lines indicate the position of the frontier molecular orbitals of the parent XF, while the solid lines indicate the changes to the FMOs upon binding of a cation or an anion to the XF.

FMO-separated XFs, provide a unique opportunity to develop responsive materials; by spatially separating HOMO and LUMO on a conjugated framework, analytes can independently address these FMOs, translating electronic into spatial information. Large changes in optical properties result upon analyte recognition. Figure 11 schematically represents the possible responses for pair wise symmetrically substituted XFs. If both positive and negatively charged species are allowed to interact with functionalized XFs, *eight different electronic responses (A-H) exhibiting unique emission colors will result*. In case **A**, coordination of an electron deficient analyte (ie a proton or metal cation) with the HOMO-

branch of an XF stabilizes the HOMO, yielding a blue-shifted emission. In **B**, binding to the LUMO-containing axis of the XF elicits a red shift emission. These effects are reversed in cases **D** and **E** where an anion or an electron releasing species interacts with the XF; here, the HOMO or the LUMO are destabilized, leading to a red shift in **D** and an expected quenching in **E**. If all four termini are bound by an analyte (**C** and **F**), only slight net shifts should be visible. In principle, either a blue or a red shift could be observed; however, in the case of **C** (**20**), we observe a slight net blue shift, while in **F** we observe a significant red shift.

Thus far, we have successfully constructed and explored cases **A-F**. Future efforts will examine further functionalization of the XF core to achieve the interesting and challenging cases **G** and **H**. In the case of **G**, addition of an electron releasing analyte to the HOMO branch and an electron deficient species to the LUMO branch, the LUMO is destabilized while the HOMO is stabilized and a dramatic blue shift is expected. In **H** we predict the opposite effect where LUMO is stabilized and HOMO is destabilized; emission in the red or near IR will result. These final examples will fully unveil the potential responses which can be registered using XFs. In the future, additional responsive diversity can be introduced with XFs if the distyryl and arylolethynyl branches are asymmetrically substituted. These efforts highlight the importance of developing new conjugated architectures.